



Figures and figure supplements

CD56 regulates human NK cell cytotoxicity through Pyk2

Justin T Gunesch et al

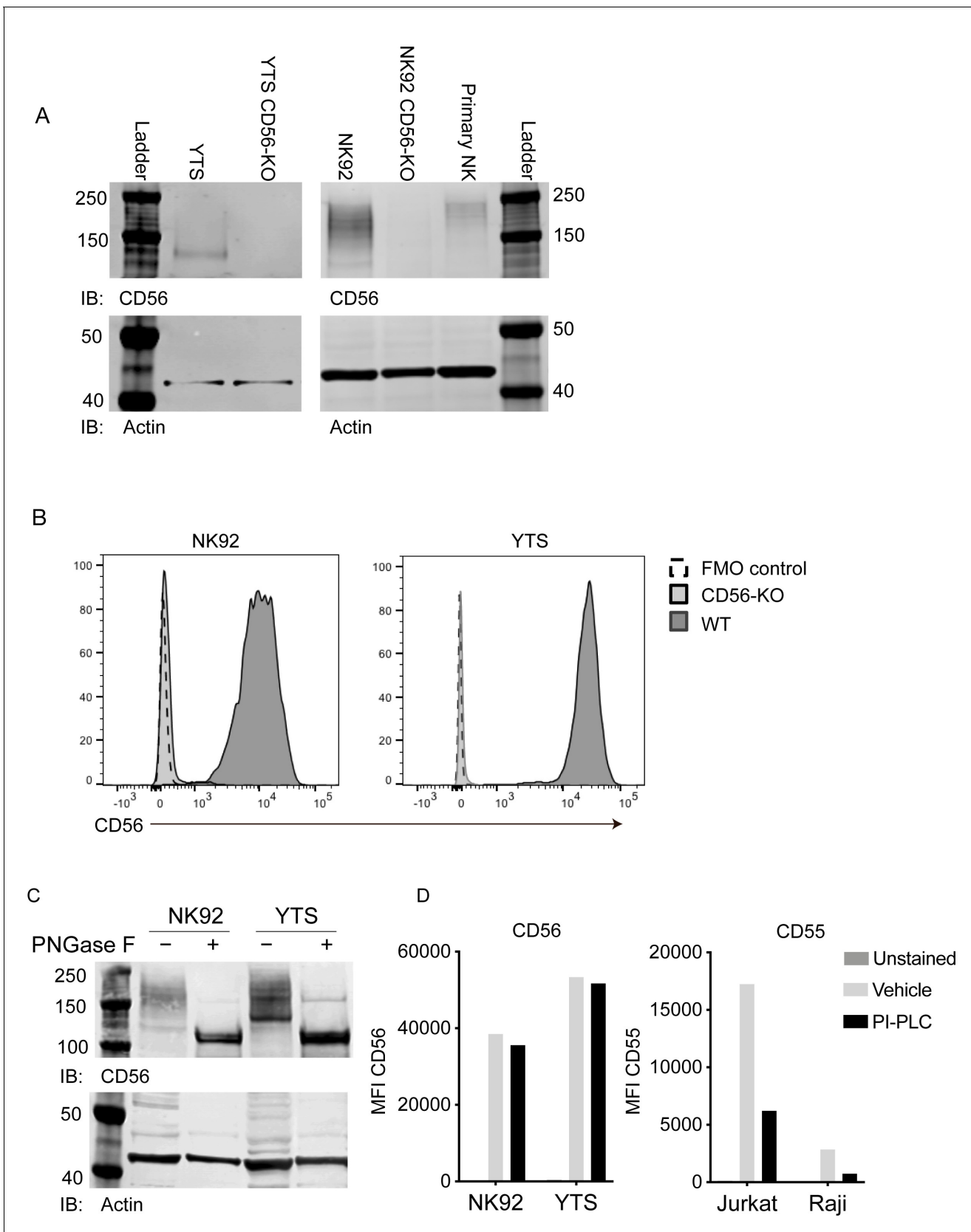


Figure 1. Validation of CD56 deletion in human NK cell lines and characterization of CD56 and its polysialylation in human NK cells. **(A)** Western blot analysis of CD56 from wild-type (WT) and CD56-knockout (KO) YTS (left) and NK92 (right) cell lines or primary human NK cells with actin as a loading control. **(B)** Flow cytometry analysis of CD56 expression in NK92 and YTS cells. **(C)** Western blot analysis of CD56 and actin in NK92 and YTS cells treated with PNGase F. **(D)** Bar graphs showing the Mean Fluorescence Intensity (MFI) of CD56 and CD55 in NK92, YTS, Jurkat, and Raji cells under Unstained, Vehicle, and PI-PLC conditions. *Figure 1 continued on next page*

Figure 1 continued

control. **(B)** Flow cytometry analysis of CD56 expression in NK92 or YTS WT (filled histogram, dark grey) or CD56-KO (filled histogram, light grey) cells compared to unstained cells (dashed line). **(C)** NK92 or YTS cells were treated with PNGase F to remove polysialic acid. Following treatment, lysates were separated by SDS-PAGE and CD56 or actin as a loading control were detected by Western blotting. **(D)** NK cell lines (left) or Jurkat or Raji cells as a positive control (right) were treated with PI-PLC to cleave GPI anchored proteins from the cell surface. PI-PLC activity was confirmed by cleavage of GPI-anchored CD55 (right). All data shown are representative of 3 technical replicates performed on different days.

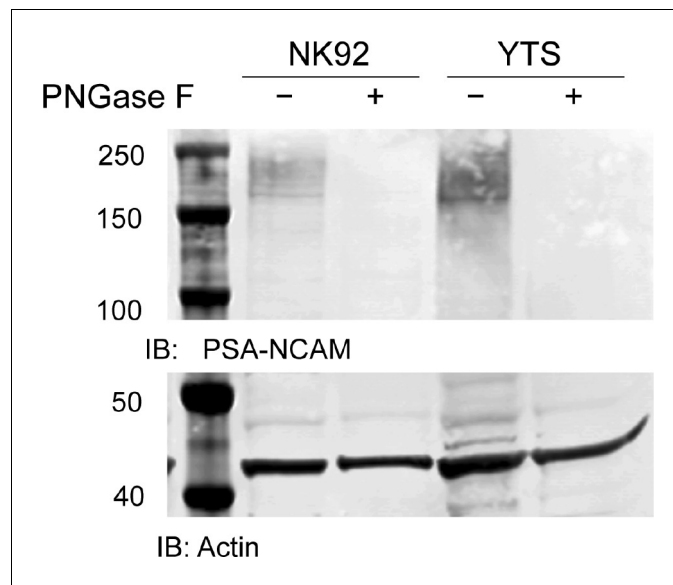


Figure 1—figure supplement 1. Expression of PSA-NCAM on human NK cell lines. NK92 or YTS cell line lysates were pre-treated with PNGase F to remove PSA-NCAM through cleavage of N-linked glycans. Following enzyme treatment, lysates from treated and untreated conditions were separated by SDS-PAGE and Western blotting with anti-PSA-NCAM antibody or actin as a loading control was performed.

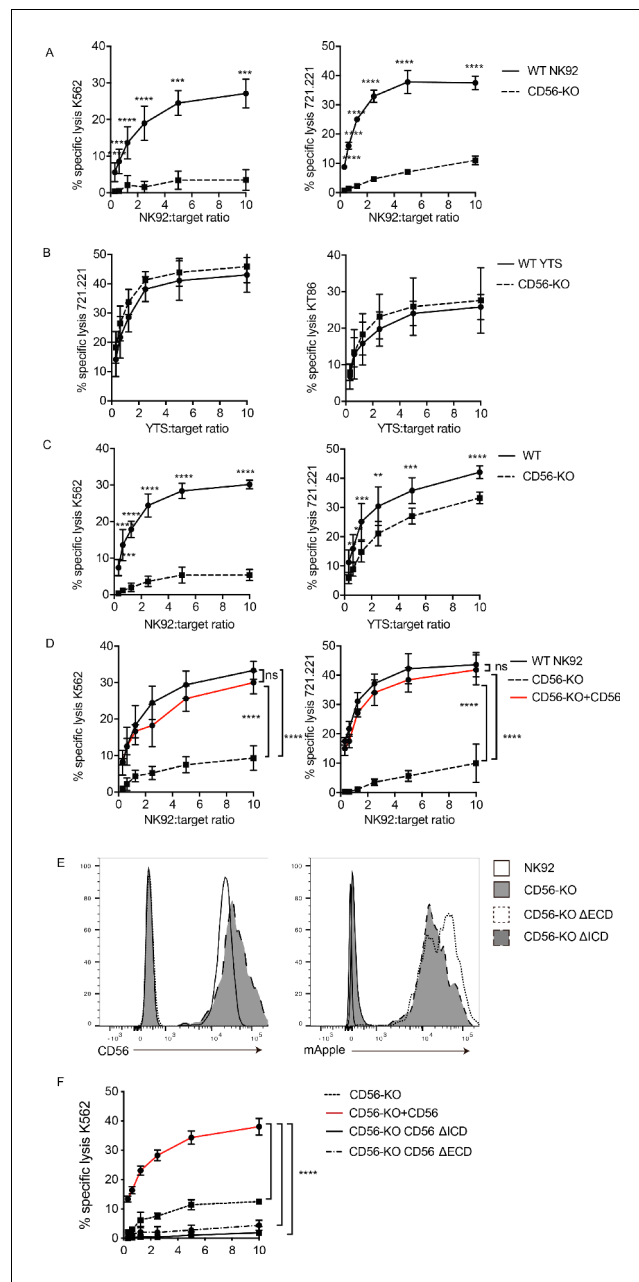


Figure 2. CD56 deletion abrogates NK92 cytotoxic function and delays YTS cytotoxicity. ⁵¹Cr-release assays were performed using NK92 (A, C, D) or YTS (B, C) WT and CD56-KO cell lines as effectors against susceptible targets. (A) 4 hr assays were performed with NK92 cell lines using K562 (left) or 721.221 (right) target cells. (B) 4 hr assays were performed with YTS cell lines using 721.221 (left) or KT86 (right) target cells. (C) 1 hr ⁵¹Cr-release assays were performed using NK92 (left) or YTS (right) cells as effectors. (D) CD56 (NCAM-140) was re-expressed in NK92 CD56-KO cells and these cells, NK92 or NK92 CD56-KO cells were used for 4 hr cytotoxicity assays against K562 (left) or 721.221 (right) target cells. (E) CD56-KO NK92 cells were transfected with chimeric CD56 constructs fused to an mApple fluorescent reporter as described in Materials and methods. Flow cytometry was used to confirm the expression of CD56 and/or mApple. (F) Cytotoxicity assays were performed with chimeric cell lines using K562 cells as targets. Mean ± S.D. of three independent experiments pooled. **p<0.01, ***p<0.001, ****p<0.0001 by Ordinary one-way ANOVA with multiple corrections test or unpaired student t-test with Welch's correction. ΔECD: chimeric construct lacking extracellular domain, ΔICD: chimeric construct lacking intracellular domain.

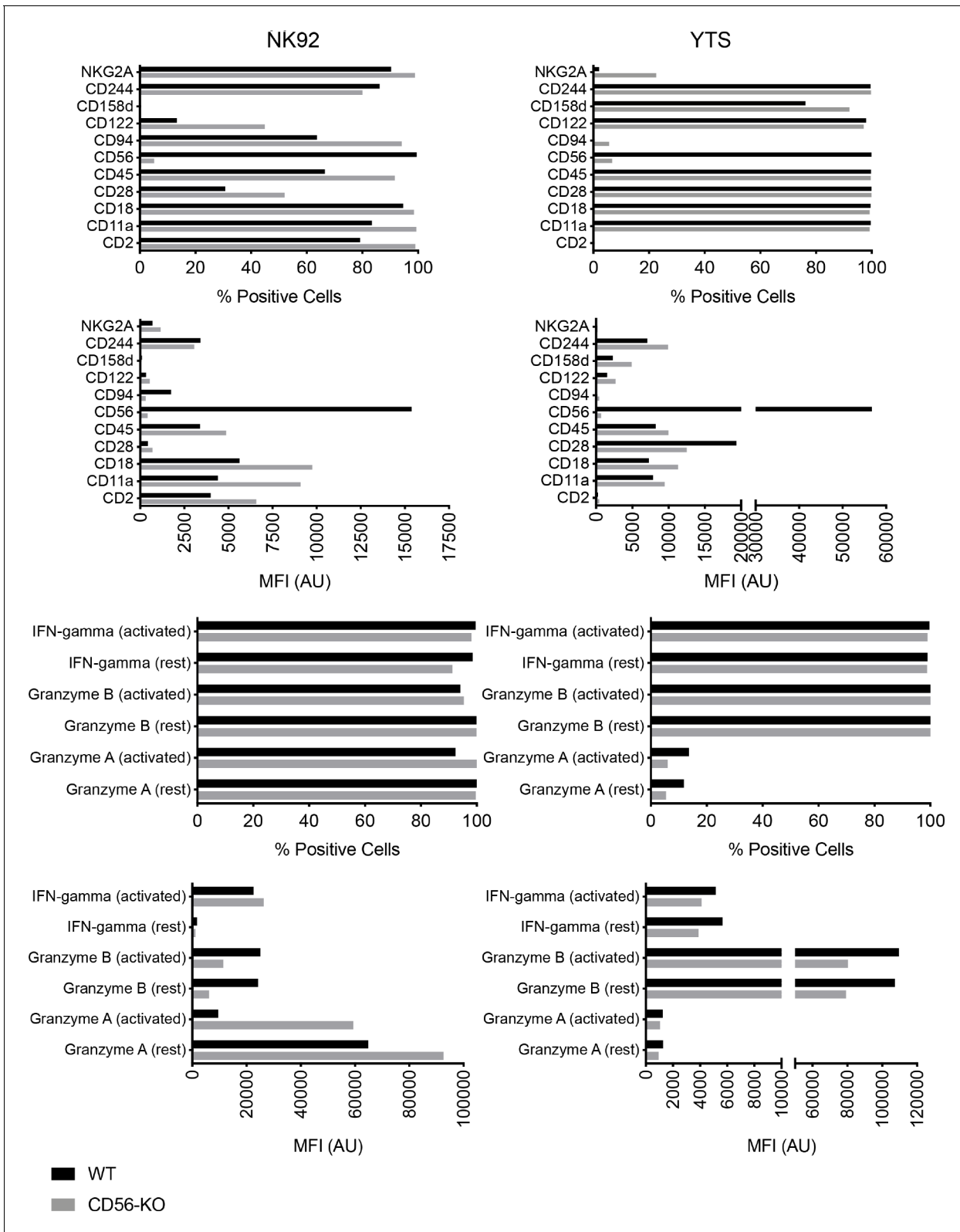


Figure 2—figure supplement 1. Phenotyping of NK cell lines by flow cytometry. NK92 and YTS WT and CD56-KO cells were analyzed for expression of cell surface receptors and intracellular effector molecules using five panels as described in Materials and methods. Effector functions were evaluated in the presence (activated) or absence (rest) of activation by PMA and ionomycin. Mean fluorescence intensity was measured and % positive cells based on fluorescence minus one gating was also calculated. Shown is one representative of 3 independent experiments.

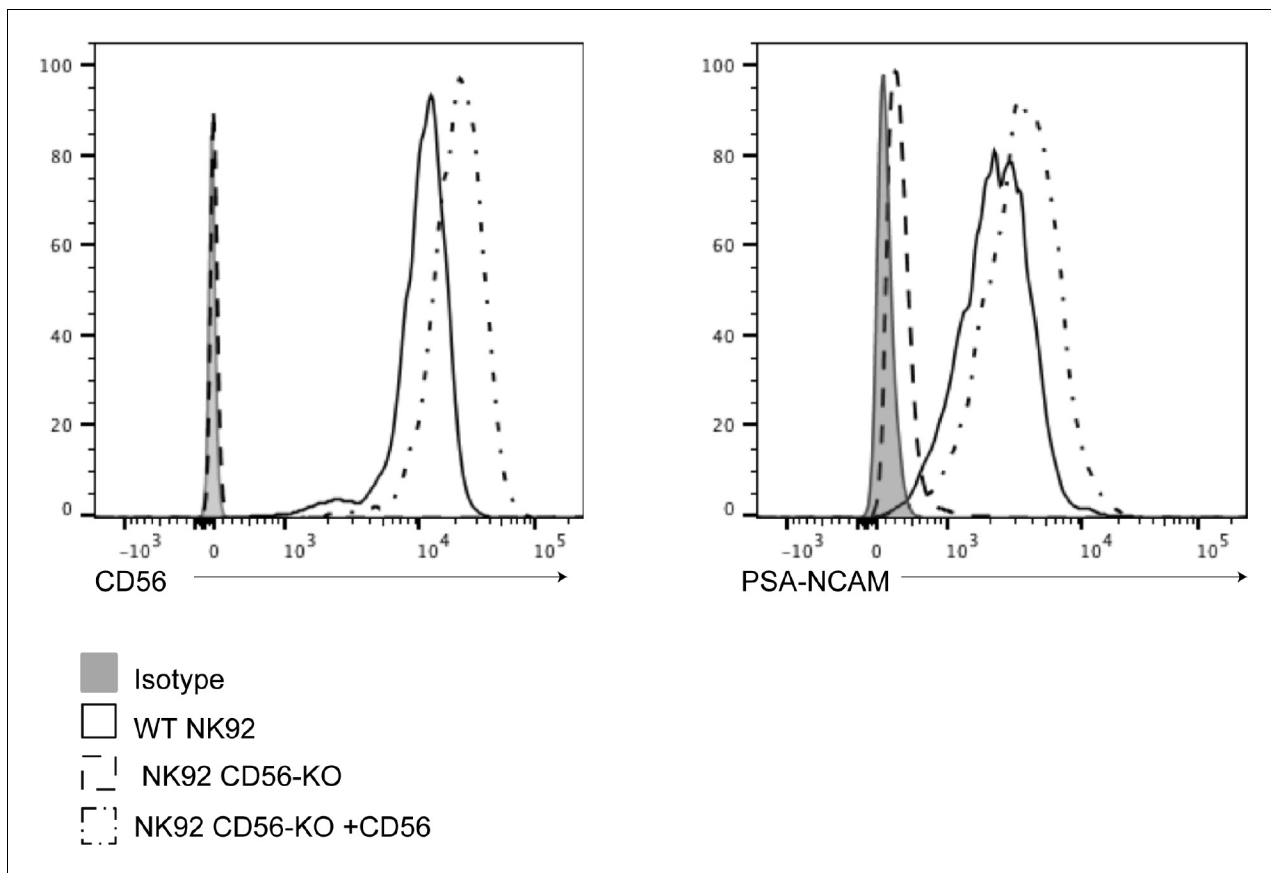


Figure 2—figure supplement 2. Re-expression of CD56 and PSA-NCAM in reconstituted NK92 cell lines. CD56 (left) or PSA-NCAM (right) were detected by flow cytometry on WT (solid line), CD56-KO (dashed line) or CD56-KO cells reconstituted with NCAM140 (dot-dashed line). Isotype antibody was used as a negative control (solid filled histogram). Shown is one representative of two independent repeats.

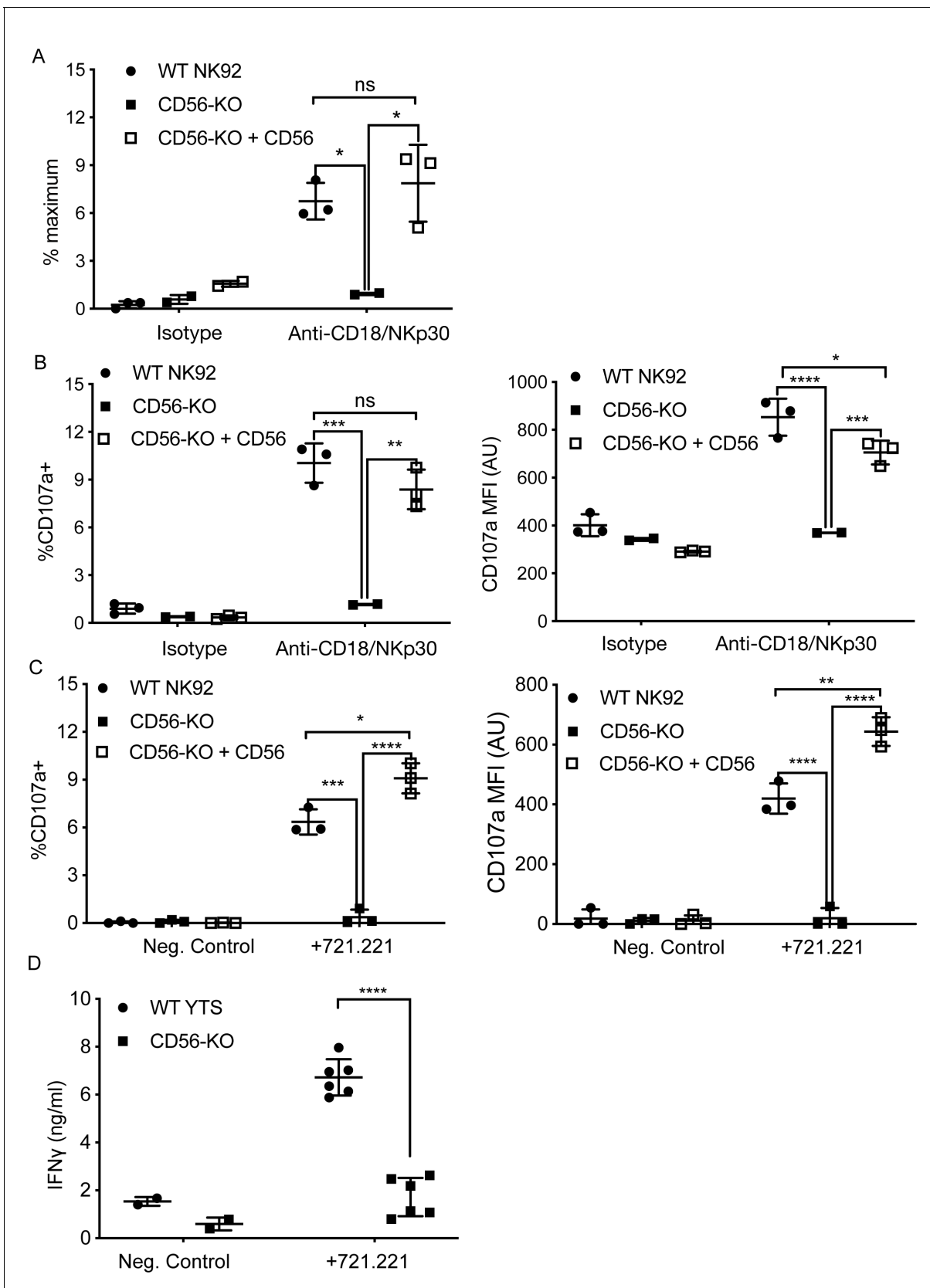


Figure 3. CD56 expression is required for exocytosis of NK92 cells. (A) WT NK92, CD56-KO or CD56-KO reconstituted cells were incubated for 60–90 min on plates pre-coated with 10 μ g/ml of anti-CD18 and anti-NKp30 antibodies. Supernatant was collected and granzyme A secretion was measured

Figure 3 continued on next page

Figure 3 continued

by a BLT esterase assay. Secretory potential was measured as a readout of the % maximum of granzyme A activity in the supernatant. (B) WT NK92, CD56-KO or CD56-KO reconstituted cells were incubated for 1–2 hr on plates pre-coated with 10 μ g/ml of anti-CD18 and anti-NKp30 antibodies. Cells were harvested and degranulation was measured by CD107a expression using flow cytometry. (C) WT NK92, CD56-KO or CD56-KO reconstituted cells were co-cultured with 721.221 target cells. Cells were harvested and CD107a expression was measured by flow cytometry. For co-culture experiments the average background of media only was subtracted from samples. Mean \pm SD. * p <0.05, ** p <0.01, *** p <0.001, **** p <0.0001 by one-way ANOVA with Tukey's multiple comparisons post-hoc test. (D) WT YTS and CD56-KO cells were incubated with 721.221 target cells at a 2:1 ratio for 22 hr. Supernatant was collected and used in a human IFN gamma ELISA. **** p <0.0001 by unpaired student t-test with Welch's correction. All data are representative of 3 independent experiments performed in duplicate or triplicate.

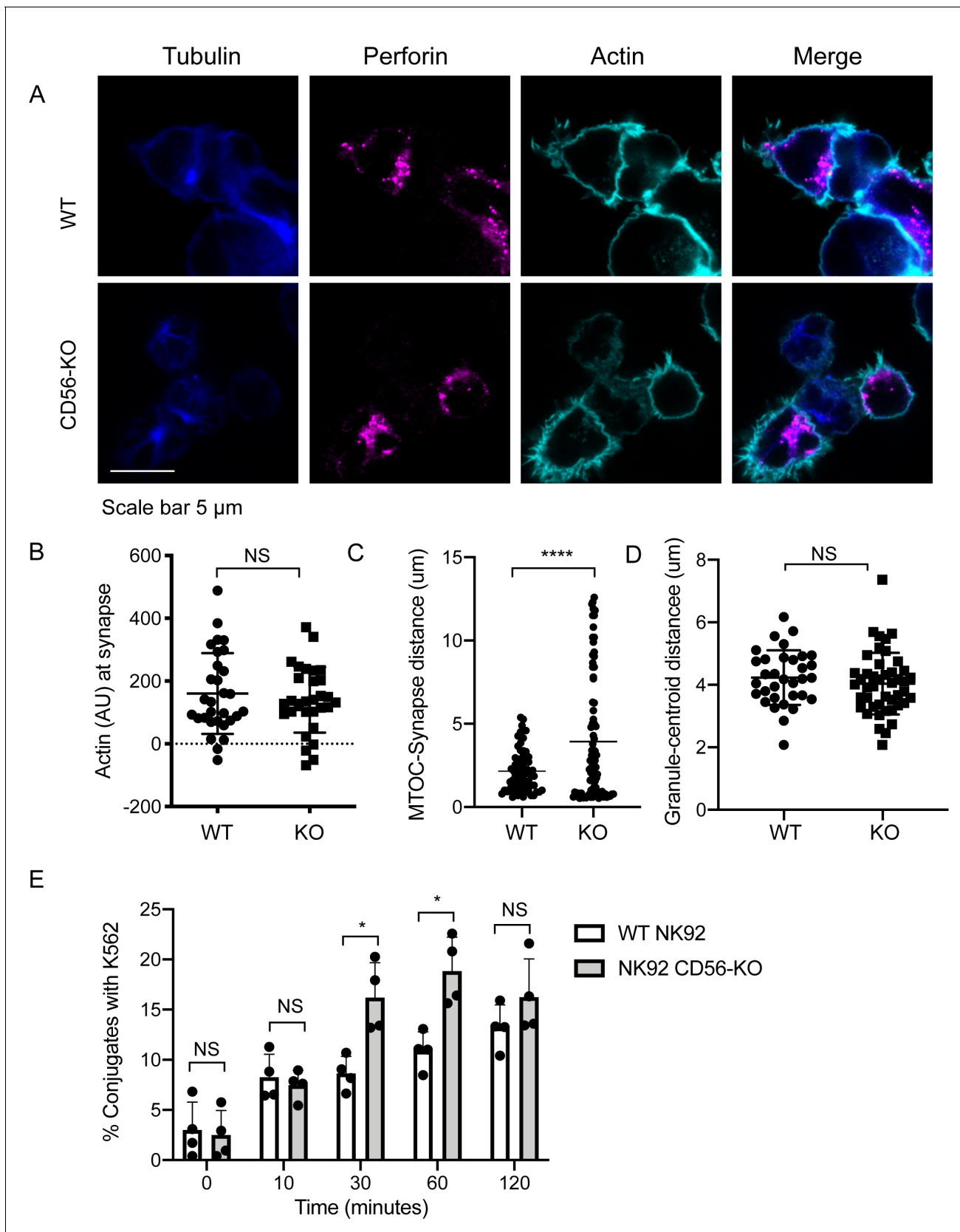


Figure 4. Impaired immune synapse formation in NK92 CD56-KO cells. WT or CD56-KO effector cells were cultured at a 2:1 ratio with K562 target cells for 45 min then fixed, immunostained and visualized by confocal microscopy. (A) Representative images from >30 cells from three independent
 Figure 4 continued on next page

Figure 4 continued

experiments immunostained as indicated. **(B)** Integrated intensity of actin at the immune synapse for WT or CD56-KO cells. Data are representative from one experiment performed three times. $n = 30, 39$. NS = not significant by unpaired t-test. **(C)** MTOC to synapse distance (μm) calculated from WT or CD56-KO conjugates. $n = 70, 83$. Data pooled from three independently replicated experiments. **(D)** Mean granule to centroid distance for WT or CD56-KO conjugates. Each data point represents the mean distance granule to centroid distance from one conjugate. $n = 33, 45$ from one representative experiment of >3 experiments. NS = not significant by unpaired T test with Welch's correction. **(E)** WT or CD56-KO NK92 effector cells were differentially labeled then conjugated at a 2:1 ratio with K562 target cells for the times indicated then fixed and analyzed by flow cytometry. The frequency of NK92-K562 conjugates was calculated for each timepoint. Each point represents a single experiment performed on different days in triplicate ($n = 4$ replicates). Error bars indicate mean \pm SD; $*p < 0.05$ by Mann-Whitney test.

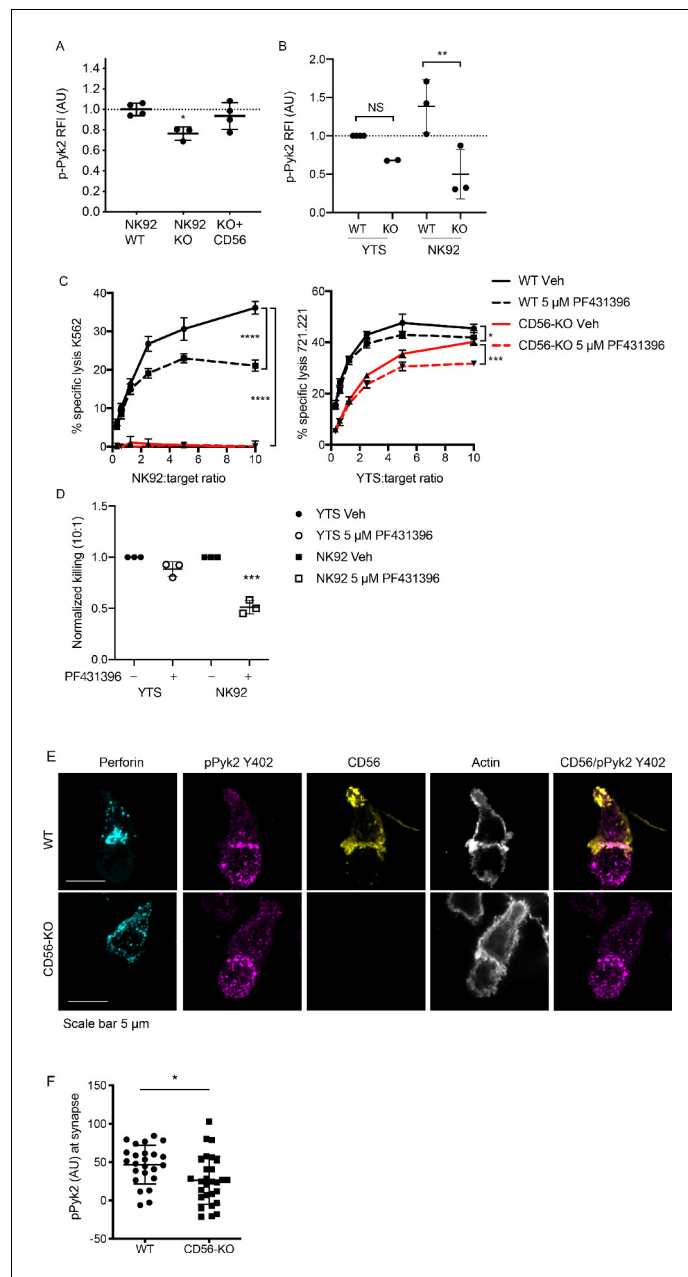


Figure 5. Phosphorylation of Pyk2 is decreased in NK92 CD56-KO cells upon activating receptor ligation. (A) NK92 WT, CD56-KO or CD56 reconstituted (KO+CD56) cells were incubated for 25–30 min on plates pre-coated with 10 $\mu\text{g}/\text{ml}$ of anti-CD18 and anti-NKp30 antibodies. Cells were permeabilized and immunostained for pPyk2 Y402 then data were acquired by flow cytometry. Relative fluorescent intensity (RFI) of pPyk2 was calculated based upon the intensity of the WT NK92 condition. Shown are the pooled data from three independent experiments. (B) WT or CD56-KO NK92 or YTS cells were permeabilized and immunostained for pPyk2 Y402 then data were acquired by flow cytometry. Shown is pooled data from 2 (YTS) or 3 (NK92) independent experiments. $**p < 0.01$ by one-way ANOVA with multiple comparisons. (C) 4 hr ^{51}Cr assays were performed with WT (black) or CD56-KO (red) NK92 cells as effectors. Assays were performed in the presence of Pyk2 inhibitor PF431396 or vehicle control (DMSO) following brief pre-incubation of effectors with inhibitor. Shown are representative data from three independent repeats. (D) Pooled data from the 10:1 effector to target cell ratio of the experiments described in (C) normalized to the WT YTS condition without inhibitor. $***p < 0.001$ by one-way ANOVA with multiple comparisons. (E) Representative confocal microscopy images of WT or CD56-KO NK92 effectors conjugated to K562 target cells in the presence of non-blocking CD56 antibody then fixed and immunostained for perforin, pPyk2 Y402 and actin. (F) Fluorescent intensity of pPyk2 Y402 at the immune synapse of WT or CD56-KO effector cells. $n = 24, 28$ from one representative experiment of 3 independent repeats.

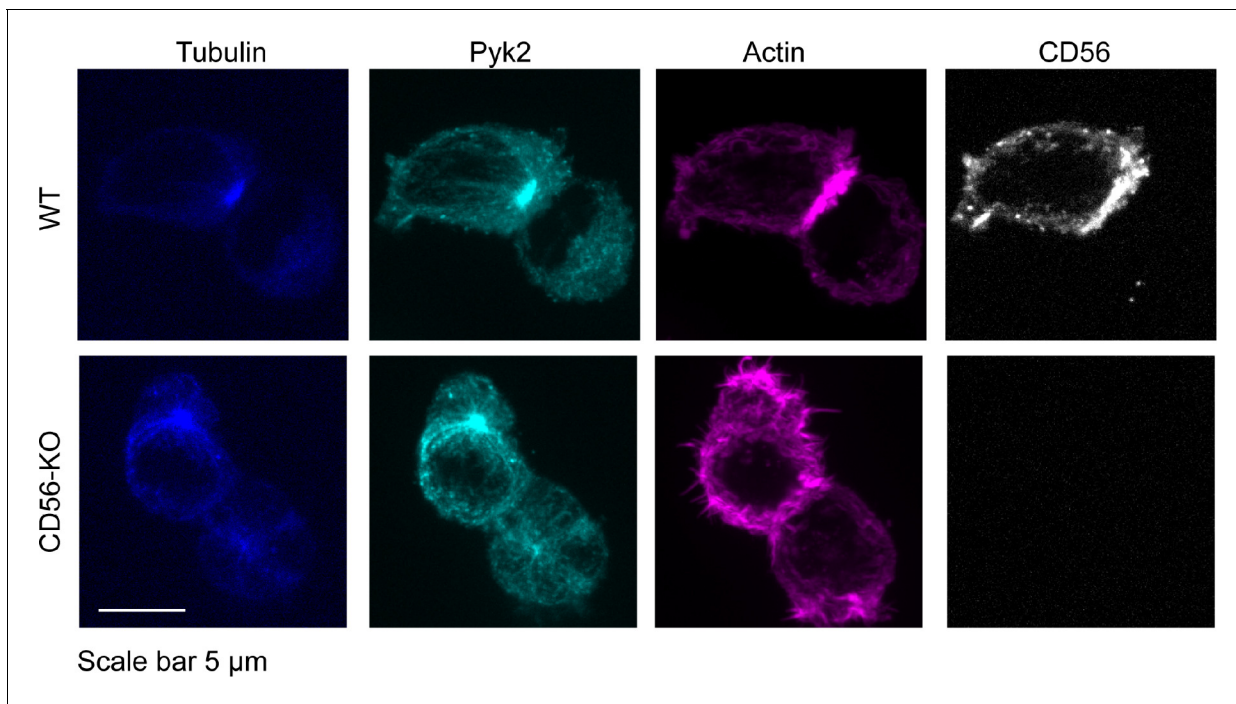


Figure 5—figure supplement 1. Detection of total Pyk2 in WT and CD56-KO cell lines. WT (top) or CD56-KO (bottom) NK92 cells were conjugated to K562 targets then fixed, permeablized and immunostained for tubulin, Pyk2, actin (phalloidin) and CD56. Images were acquired on a spinning disk confocal microscope. Shown is one representative of 60 cells from two independent technical replicates.

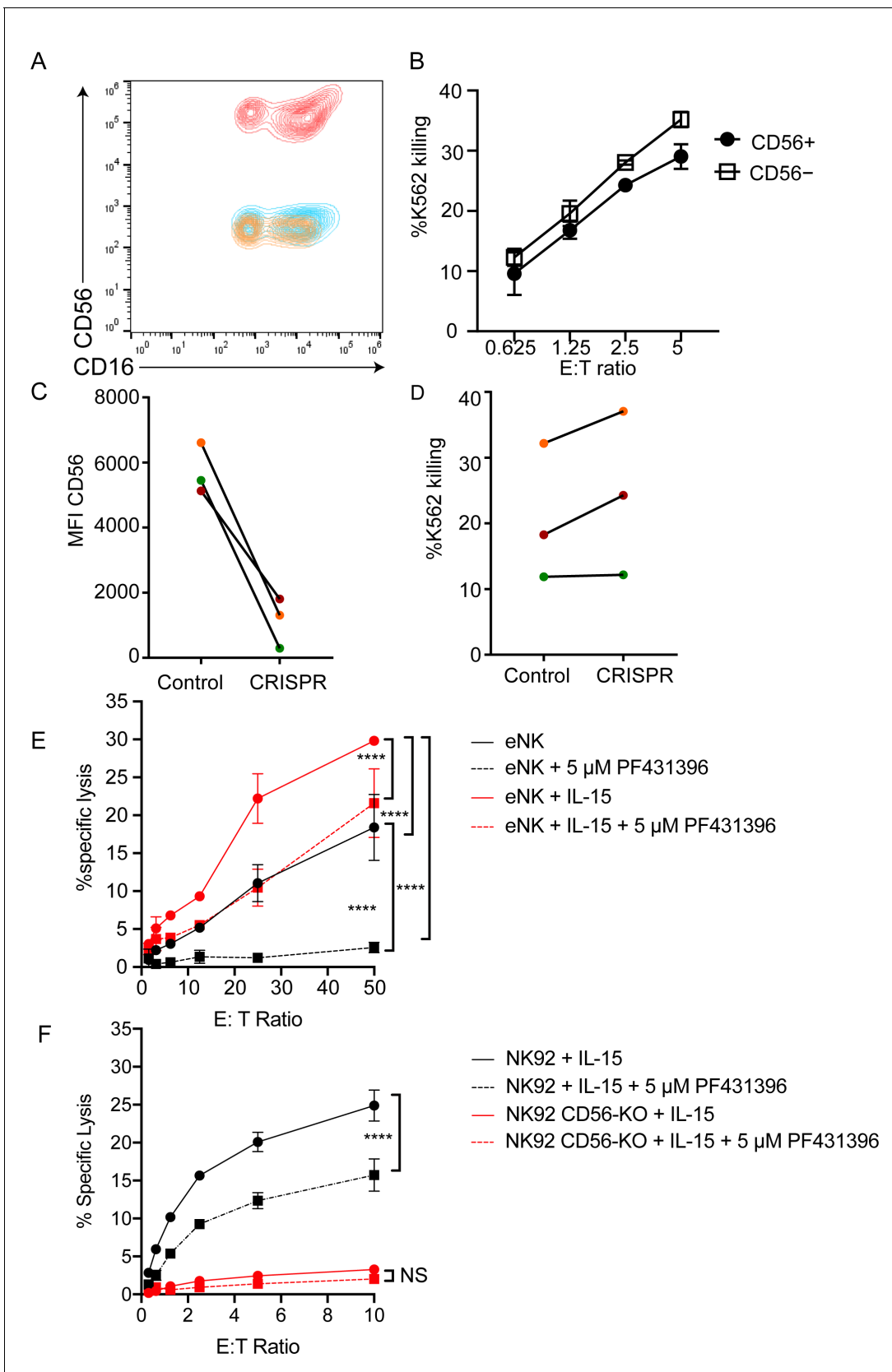


Figure 6. CD56-deficient primary NK cells retain lytic function. Primary NK cells were isolated and allowed to rest overnight in the presence of low-dose IL-15 prior to delivery of CD56 CRISPR-Cas9. Cells were further expanded in the presence of 25 ng/ml IL-15 for 15 days and cytotoxicity against K562
 Figure 6 continued on next page

Figure 6 continued

targets was measured. (A) Representative FACS plot of CD56-deficient (blue) or control primary cells (red) after 15 days of IL-15 expansion. Shown also is the fluorescence minus one control (yellow). (B) K562 target cell lysis by primary NK cells shown in (A). (C) Control or CD56-deficient NK cells from three healthy donors were incubated for 1 week after CD56 CRISPR-Cas9 delivery in 25 ng/mL IL-15 then cells were isolated by FACS and cultured for an additional 8 days and the MFI of CD56 was measured by flow cytometry. (D) Specific lysis of K562 target cells by isolated and expanded CD56^{bright} NK cells from the three healthy donors shown in (C). (E) Primary NK cells were incubated and expanded for 14 days in the presence of 50 ng/ml IL-15 then cytotoxicity against K562 target cells was tested in the presence or absence of Pyk2 inhibitor PF431396. Freshly isolated, non-expanded NK cells were used as a control and similarly treated with PF431396. (F) WT or CD56-KO NK92 cells were incubated for 7 days in the presence of 50 ng/ml IL-15 then cytotoxicity was tested in the presence or absence of PF431396. Shown is one representative experiment from three independent biological repeats. Error bars represent 3 technical repeats, SEM.

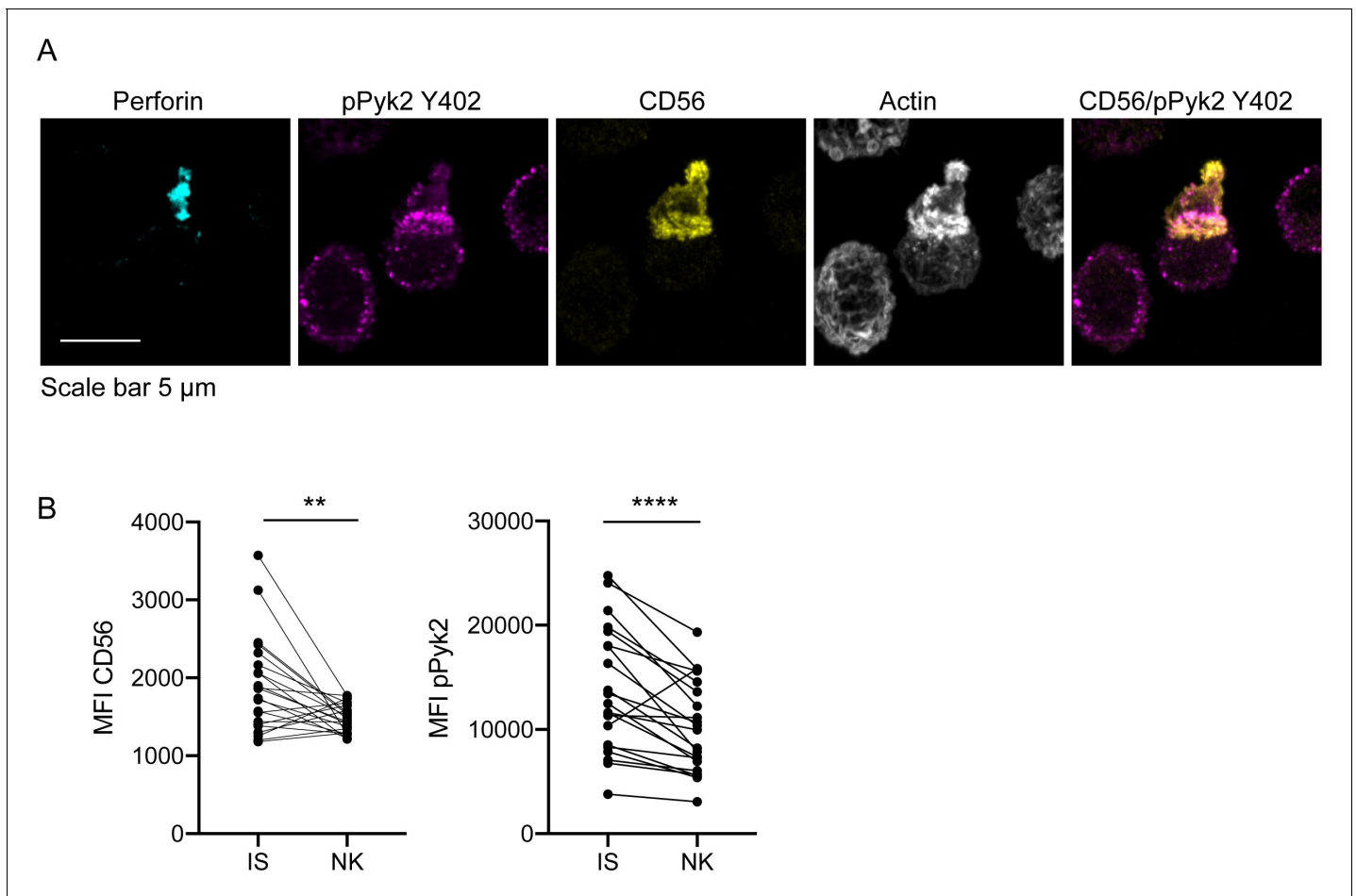


Figure 7. CD56 co-localizes with pPyk2 Y402 to the immune synapse in primary human NK cells. Primary NK cells were enriched from peripheral blood then incubated with K562 target cells for 45 min on poly-L-lysine coated coverslips in the presence of non-blocking anti-CD56 antibody. Following incubation cells were fixed, permeabilized, and immunostained for pPyk2 Y402 (magenta), perforin (cyan) and actin (phalloidin, greyscale). 3D volumetric images were acquired by spinning disk confocal microscopy. (A) Representative images from one of three healthy donors. Shown is a maximum projection of 13 planes taken with 0.5 μ m steps. (B) Fluorescence intensity of CD56 (left) or pPyk2 Y402 (right) measured at the synaptic (IS) or non-synaptic (NK) cell cortex of primary NK cells conjugated to target cells. $n = 22$ from one independent experiment of 3 using three different healthy donors. ** $p < 0.005$, **** $p < 0.0001$ by paired t-test.